PHYS 7398
Pulsed Nuclear Magnetic Resonance

Amanda Nowicki
Department of Physics and Astronomy, Louisiana State University
(Dated: February 24, 2025)

The spin-lattice relaxation time (T_1) and spin-spin relaxation time (T_2) of glycerin-water mixtures and undiluted mineral oil were measured using the TeachSpin PS1-A Pulsed Nuclear Magnetic Resonance (PNMR) spectrometer. The experiment utilized a two-pulse sequence to analyze magnetization decay, with data collected using a pickup coil and oscilloscope. Samples of undiluted glycerin, undiluted mineral oil, and glycerin-water mixtures at varying concentrations were examined over different delay times ranging from 10 to 400 ms to investigate the effects of viscosity and molecular interactions on relaxation times. Linearized magnetization decay plots were used to extract relaxation values, with the T_1 of undiluted glycerin, 3:1 glycerin-water mixture, 2:1 glycerin-water mixture, 1:1 glycerin-water mixture, and undiluted mineral oil found to be 20.7 ± 0.6 ms, 24.0 ± 1.0 ms, 76.0 ± 3.0 ms, and 213.0 ± 10.0, and 68.0 ± 2.0 ms,respectively. Additionally, the T_2 of the same samples were found to be 11.08 ± 0.3 ms, 21.9 ± 0.2 ms, 88.1 ± 0.5 ms, and 204.0 ± 2.0 ms, 15.5 ± 0.1 ms, respectively. The measured values for undiluted mineral oil and glycerin fall within the expected range for these substances, while the relaxation times for the glycerin-water mixtures follow the anticipated trend, with higher water content generally resulting in longer relaxation times.

I. INTRODUCTION

Nuclear Magnetic Resonance (NMR) is a widely used spectroscopic technique for studying the magnetic properties of atomic nuclei. The principle of NMR is based on the interaction between nuclear spins and an external magnetic field. When a sample is placed in a static magnetic field (B_0), nuclear spins align with or against the field, creating a net magnetization along the *z-axis*. This magnetization can be perturbed using a radiofrequency (RF) pulse, causing the spins to precess about B_0 at the Larmor frequency, given by

$$\omega_0 = \gamma B_0$$

where γ is the gyromagnetic radio, a nucleus-dependent constant.

Pulsed NMR (PNMR) utilizes short RF pulses to rotate the net magnetization away from equilibrium, and the subsequent relaxation processes are measured. Two primary relaxation mechanisms are observed:

1. Spin-lattice Relaxation Time (T_1)

Spin-lattice relaxation time (T_1) describes the recovery of the longitudinal magnetization (M_z) along B_0 due to energy exchange between the nuclear spins and their surrounding environment, known as the "lattice". This relaxation follows the equation:

$$M_z(t) = M_0(1 - 2e^{-\tau/T_1}) \tag{1}$$

where (M_0) is the equilibrium magnetization.

2. Spin-Spin Relaxation Time (T_2)

Spin-spin relaxation time (T_2) describes the dephasing of transverse magnetization ($M_{x,y}$) due to spin-spin interactions and field inhomogeneities. This process follows and exponential decay:

$$M_{x,y}(t) = M_0 e^{-2\tau/T_2}) \tag{2}$$

where τ is the time delay between the RF pulses in the pulse sequence.

The measurement of T_1 and T_2 provides insight into molecular motion, viscosity, and intermolecular interactions within a sample [1].

II. PROCEDURE

A. Experimental Setup

The experiment was conducted using the TeachSpin PS1-A Pulsed NMR Spectrometer. The system consists of a permanent magnet that provides a static magnetic field B_0, a pulse programmer that generates RF pulses, and a pickup coil that detects the resulting magnetization signals. An oscilloscope was used to monitor and record the Free Induction Decay (FID) and spin echoes. The schematics for the experimental setup are shown in Figure 1.

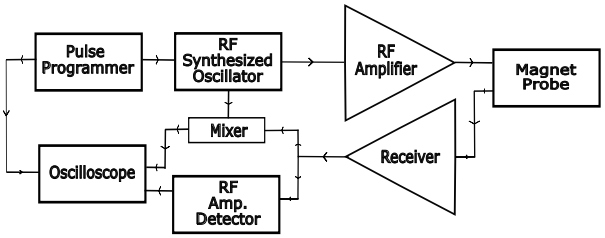

FIG. 1: Schematic of the experimental setup.

B. Sample Preparation

Five different liquid samples were prepared to study the effects of viscosity and molecular interactions on nuclear spin relaxation. Each mixed sample contained an approximate volume ratio of glycerin to water, mixed manually. Details of each sample composition are shown in Table 1.

TABLE I: Composition of samples used in the experiment. Percentages are approximate.

Sample	Glycerin %	Water %	Notes
Undiluted glycerin	100	0	Pure glycerin
3:1 glycerin-water	75	25	Approximate ratio
2:1 glycerin-water	67	33	Approximate ratio
1:1 glycerin-water	50	50	Equal parts
Mineral oil	0	0	Pure mineral oil

The volume percentages were estimated based on measurement markings and manual pipetting, so slight variations in concentration are expected. A rubber O-ring was used to adjust the height of the sample in the probe. Approximately 6 mm of total sample volume was used in each case to maintain consistency across measurements. Figure 2 shows the sample vial setup.

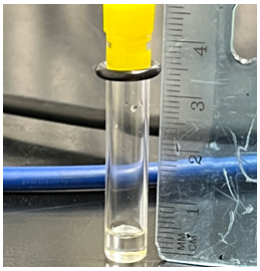

FIG. 2: Sample vial with sample and o-ring.

C. Finding Resonance Frequency

Before collecting relaxation time data, the system was tuned for each sample to ensure that the oscillator frequency matched the Larmor frequency of the protons of the sample. This was necessary to maximize the FID signal and ensure accurate measurements.

The TeachSpin PS1-A PNMR spectrometer was used for this process. The oscilloscope was set up to display both the FID signal and the RF signal from the 15.14 MHz oscillator module. The oscillator frequency was adjusted while observing the RF signal on the oscilloscope. When the RF beats flattened out and the FID signal reached its maximum amplitude, resonance was achieved. Figure 3 illustrates the contrast between the untuned and tuned frequency for any given sample.

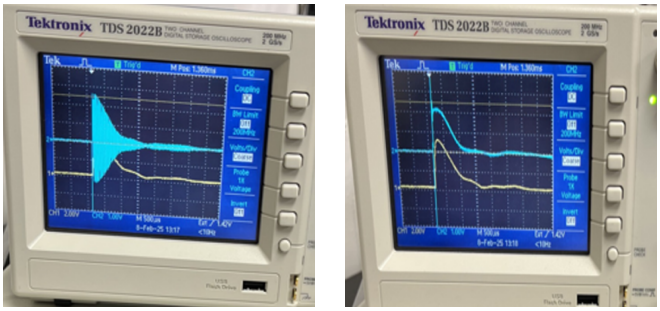

(a) Untuned frequency (b) Tuned frequency

FIG. 3: Oscilloscope displays showing an untuned (a) signal and a tuned (b) signal.

After tuning the frequency, the sample position was optimized to ensure it was fully within the homogeneous region of the static magnetic field. This was done by making small adjustments to the sample's position within the probe while monitoring the FID signal until a maximum response was observed. Finally, the tuning knob on the receiver module was adjusted to further maximize the signal strength. Once these steps were completed for each sample, data collection for T_1 and T_2 measurements began.

D. Measurement of T_1

Before measuring the spin-lattice relaxation time T_1, the pulse widths were calibrated to ensure accurate excitation of nuclear spins. The TeachSpin PS1-A PNMR spectrometer allows for manual adjustment of pulse durations, which was necessary to generate precise 180° and 90° pulses. A 180° was confirmed by minimizing the initial FID signal, while a 90° pulse was optimized to maximize the recorded signal amplitude. An illustration is shown in Figure 4(b).

The spin-lattice relaxation time T_1 was measured using an inversion-recovery pulse sequence. A 180° pulse

was applied to invert the longitudinal magnetization M_z, followed by a variable delay time τ. A 90° pulse was then applied to rotate the magnetization into the transverse plane, and the signal was recorded using the pickup coil. The amplitude of the detected 90° signal was measured as a function of τ, and T_1 was extracted by fitting the data to the exponential recovery Equation (1).

E. Measurement of T_2

Similarly to T_1, the pulse widths were first calibrated to ensure proper excitation and rephasing of nuclear spins. The 90° pulse was tuned to maximize the initial FID signal, while the 180° pulse was optimized to maximize the amplitude of the spin-echo signal. An illustration is shown in Figure 4(b).

The spin-spin relaxation time T_2 was measured using a spin-echo pulse sequence. A 90° pulse was applied to rotate the magnetization into the transverse plane, followed by a delay τ. A 180° pulse was then applied to rephase the spins, producing a spin-echo signal. The height of the spin-echo was recorded for different values of τ, and T_2 was determined by fitting the decay of the echo amplitude to Equation (2).

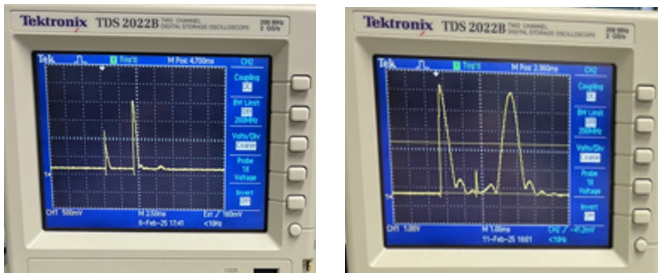

(a) Pulses for T_1 measurement

(b) Pulses for T_2 measurement

FIG. 4: Oscilloscope displays showing pulses for T_1 (a) and T_2 (b) measurements.

III. ANALYSIS AND RESULTS

Data was linearized to simplify the extraction of relaxation times and improve the accuracy of fitting. The spin-lattice relaxation time T_1 follows an exponential recovery, as shown in Equation (1). By taking the natural logarithm of both sides, we obtain a linear form:

$$ln(1 - \frac{M_z}{M_0}) = -\frac{t}{T_1} \tag{3}$$

which allows T_1 to be determined from the slope of a linear regression fit.

Magnetization values were recorded at various delay times for each sample. The data was then transformed into its linearized form according to Equation (3), enabling T_1 to be extracted from the slope of the best-fit line. The resulting linearized plots for each sample are shown in Figures 5-9.

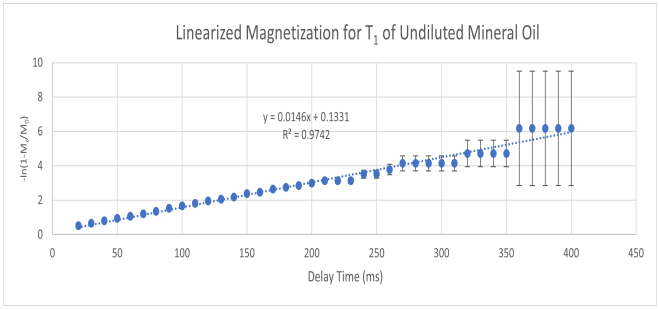

FIG. 5: Data for T_1 of undiluted mineral oil sample.

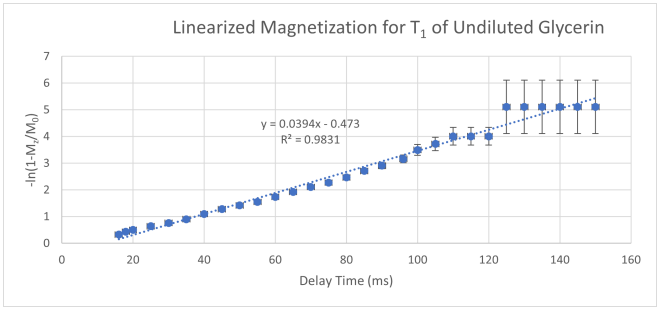

FIG. 6: Data for T_1 of undiluted glycerin sample.

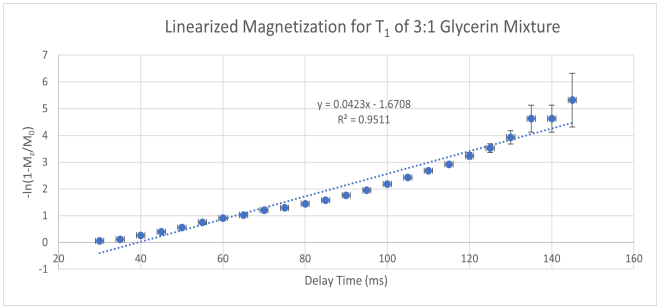

FIG. 7: Data for T_1 of 3:1 glycerin-water sample.

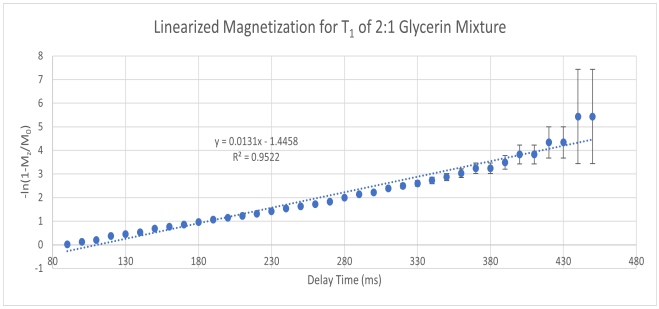

FIG. 8: Data for T_1 of 2:1 glycerin-water sample.

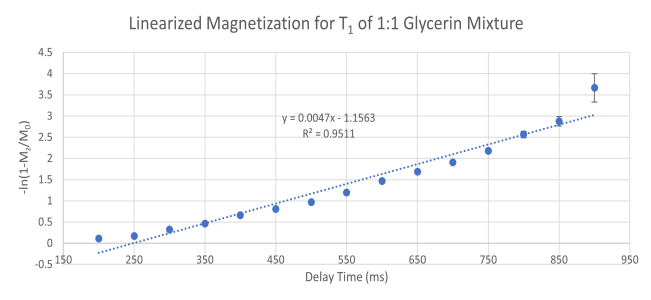

FIG. 9: Data for T_1 of 1:1 glycerin-water sample.

Similarly, the spin-spin relaxation time T_2 follows an exponential decay, as described by Equation (2). By taking the natural logarithm of both sides, we obtain a linear form:

$$ln(\frac{M_{x,y}}{M_0}) = -\frac{2\tau}{T_2} \tag{4}$$

which allows T_2 to be determined from the slope of a linear regression fit.

Magnetization values were recorded at various delay times τ for each sample. The data was then transformed into its linearized form according to Equation (4), enabling T_2 to be extracted from the slope of the best-fit line. The resulting linearized plots for each sample are shown in Figures 10-14.

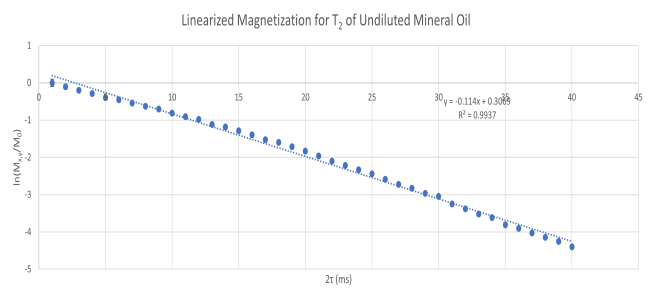

FIG. 10: Data for T_2 of undiluted mineral oil sample.

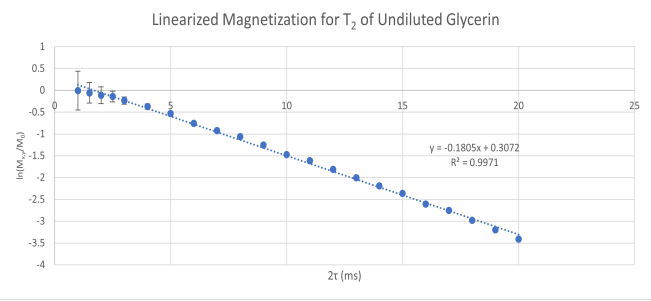

FIG. 11: Data for T_2 of undiluted glycerin sample.

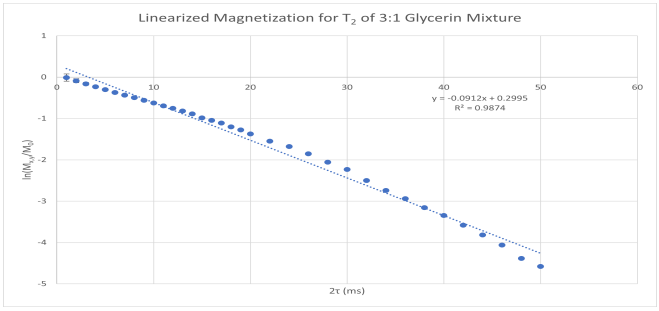

FIG. 12: Data for T_2 of 3:1 glycerin-water sample.

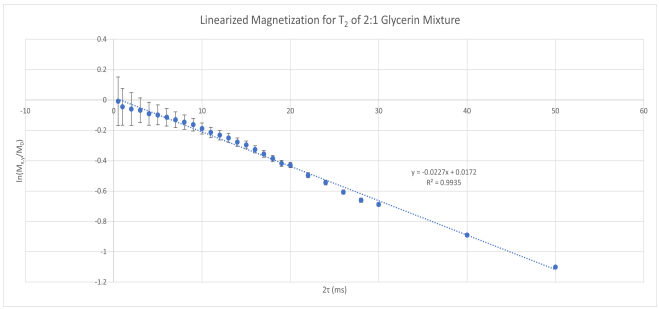

FIG. 13: Data for T_2 of 2:1 glycerin-water sample.

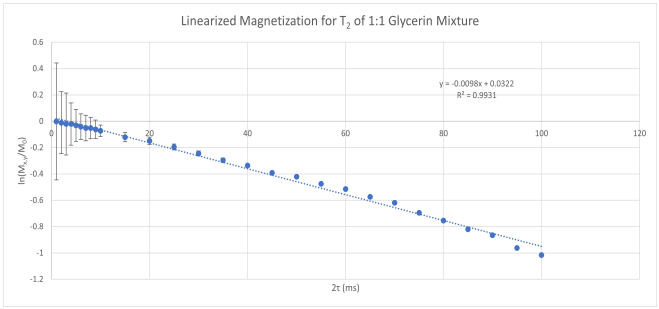

FIG. 14: Data for T_2 of 1:1 glycerin-water sample.

A. Error Calculation and Uncertainties

The error bars in our T_1 and T_2 measurements were obtained using the equation:

$$\delta V = \frac{0.02}{V_{max} - V}$$

where 0.02 V represents the resolution of the oscilloscope, V_{max} is the maximum recorded voltage for a given dataset, and V is the measured voltage at a particular delay time.

This approach accounts for the increasing difficulty in resolving small voltage changes as the signal approaches equilibrium. However, the effect of this error model differs for T_1 and T_2 due to the nature of their respective decay processes.

For T_1, the error bars are small at short delay times and increase as magnetization approaches equilibrium. This is due to the inverse relationship in our error equation, which causes uncertainties to grow as V approaches V_{max}. Additionally, as the magnetization stabilizes, the rate of signal change slows, making small voltage fluctuations more significant in relative terms. The oscilloscope's resolution further amplifies this effect, as its fixed measurement accuracy becomes a dominant source of uncertainty when the signal change per time step is minimal. As a result, the increasing error bars at longer delay times in T_1 measurements are expected and do not indicate a flaw in the data but rather reflect the inherent limitations of our measurement system.

In contrast, the T_2 data exhibits the largest error bars at early delay times rather than near equilibrium. This is primarily due to low signal-to-noise ratio (SNR) at short times, where the spin-echo signal is strongest but more susceptible to phase and pulse timing fluctuations. Small variations in the RF pulse width or phase coherence can introduce significant inconsistencies in early-time measurements, leading to greater uncertainty. Additionally, while the oscilloscope resolution still influences errors, at early times, the measured voltage is farthest from V_{max}, and rapid initial signal decay can make small voltage differences disproportionately impactful. Consequently, the T_2 error bars decrease over time as the signal decays and measurements become more stable.

After processing the data for all five samples, the values for T_1 and T_2 were determined by analyzing the slopes of the best-fit lines in their respective linearized plots. The extracted values, along with their associated uncertainties and χ^2 goodness-of-fit values, are presented in Tables II and III.

TABLE II: Measured T_1 values with uncertainties and χ^2 for samples.

Sample	T_1 (ms)	χ^2
Undiluted glycerin	20.7 ± 0.6	3.095
3:1 glycerin-water	24.0 ± 1.0	2180.0
2:1 glycerin-water	76.0 ± 3.0	33.167
1:1 glycerin-water	213.0 ± 10.0	43.342
Mineral oil	68.0 ± 2.0	3.095

TABLE III: Measured T_2 values with uncertainties and χ^2 for samples.

Sample	T_2 (ms)	χ^2
Undiluted glycerin	11.08 ± 0.3	0.301
3:1 glycerin-water	21.9 ± 0.2	502.53
2:1 glycerin-water	88.1 ± 0.5	1471000.0
1:1 glycerin-water	204.0 ± 2.0	0.581
Mineral oil	15.5 ± 0.1	1450.0

IV. DISCUSSIONS AND CONCLUSIONS

This experiment successfully measured the spin-lattice T_1 and spin-spin T_2 relaxation times for undiluted mineral oil, undiluted glycerin, and three glycerin-water mixtures using pulsed nuclear magnetic resonance (PNMR). The data followed the expected trends, and the extracted relaxation times were consistent with theoretical expectations and previously reported values.

The results indicate a strong dependence of relaxation times on sample composition. The longest T_1 value was observed for the 1:1 glycerin-water mixture (213.0 ± 10.0 ms), while the shortest T_1 value was measured for undiluted glycerin (20.7 ± 0.6 ms). This trend aligns with the known relationship between molecular motion and spin-lattice relaxation: samples with higher water content exhibit longer T_1 values due to increased molecular mobility and weaker dipole interactions [2]. Conversely, undiluted glycerin, with its high viscosity and strong intermolecular hydrogen bonding, leads to faster energy transfer between nuclear spins and the surrounding lattice, resulting in shorter T_1 values.

A similar pattern was observed in the T_2 measurements. The 1:1 glycerin-water mixture had the longest T_2 value (204.0 ± 2.0 ms), while undiluted glycerin exhibited the shortest T_2 value (11.09 ± 0.3 ms). The increase in T_2 with higher water content reflects a reduction in dipole interactions, which slow the dephasing of transverse magnetization. In contrast, the restricted molecular motion in viscous samples leads to rapid dephasing, lowering the T_2 value.

The χ^2 values varied widely across the samples, with the highest observed for the T_2 measurement of the 2:1 glycerin-water mixture ($\chi^2 = 1.47 \times 10^6$). This suggests that in some cases, measurement uncertainties may have been underestimated, or additional factors, such as sample inhomogeneities, magnetic field variations, and instrumental noise, contributed to deviations from the expected behavior [3].

Another potential source of error is RF interference. The experiment was conducted in an environment where external RF signals, such as those from the nearby KLSU station, could have affected the PNMR setup. Although the station broadcasts well above the 15.14 MHz range used in this experiment, nonlinearities in the power amplifier module may have introduced unwanted scaling effects. Some oscilloscope traces showed evidence of oscillatory behavior even after frequency tuning, suggesting that RF interference could have influenced certain measurements. Future experiments could mitigate this by performing measurements in a Faraday cage or using improved RF shielding techniques [4].

Additionally, sample placement within the NMR probe plays a crucial role in data accuracy. The uniformity of the applied magnetic field is critical for consistent relaxation time measurements. If a portion of the sample extended beyond the homogeneous region, relaxation dynamics could be affected. Careful alignment of the sam-

ple probe and repeated measurements helped minimize this effect.

Beyond fundamental research, NMR relaxation measurements have direct applications in medical imaging (MRI), material science, and chemical analysis. Understanding how relaxation times vary with viscosity and molecular composition is essential for designing better contrast agents in MRI and improving industrial fluid characterization techniques.

This experiment demonstrated that T_1 and T_2 relaxation times are strongly influenced by sample composition, with increasing water content leading to longer relaxation times due to reduced intermolecular interactions and increased molecular mobility. The data were consistent with theoretical expectations, despite some sources of uncertainty. These results highlight the importance of viscosity, dipole interactions, and external factors in determining relaxation behavior, reinforcing the utility of PNMR in studying molecular dynamics.

V. ACKNOWLEDGMENTS

I would like to thank Dr. Prosper Ngabonziza for his assistance and instruction throughout the lab. I also like to thank to my lab partner, Daniel Carpenter, for his hard work, patience, and contributions during the experiment. Additionally, I would like to thank Teach-Spin CEO Jonathan Reichert and Dr. Martin Tzanov for their time and support in system diagnostics. Finally, I would like to thank Cullen Domangue and the staff of the Electronics Development Group for their assistance with equipment repair.

[1] TeachSpin PS1-A Pulse NMR Spectrometer Instruction Manual, TeachSpin Inc., 1995.

[2] Y. Kim, "Pulsed NMR: Relaxation Times as a Function of Viscosity and Impurities," 2012.

[3] H. Y. Carr and E. M. Purcell, "Effects of Diffusion on Free Precession in Nuclear Magnetic Resonance Experiments,"Phys. Rev. 94, 630 (1954).

[4] Ibrahim, M., Pardi, C. I., Brown, T. W. C., and McDonald, P. J (2018). Active elimination of radio frequency interference for improved signal-to-noise ratio for in-situ NMR experiments in strong magnetic field gradients. Journal of Magnetic Resonance, 287, 99–109. https://doi.org/10.1016/j.jmr.2018.01.002